Journal of Power Sources 192 (2009) 316–323

Contents lists available at ScienceDirect

Journal of Power Sources

journal homepage: www.elsevier.com/locate/jpowsour

Ionic conductivity improvement in primary pores of fuel cell catalyst layers: Electropolymerization of *m*-aminobenzenesulfonic acid and its effect on the performance

Satoshi Tominaka [1], Kazuya Goto, Toshiyuki Momma, Tetsuya Osaka *

Department of Applied Chemistry, Graduate School of Advanced Science and Engineering, Waseda University, Okubo 3-4-1, Shinjuku, Tokyo 169-8555, Japan

ARTICLE INFO

Article history:
Received 3 December 2008
Received in revised form 10 February 2009
Accepted 8 March 2009
Available online 19 March 2009

Keywords:
Fuel cells
Catalyst layers
Electrochemical impedance spectroscopy
Ionic conductivity
Electropolymerization

ABSTRACT

Catalyst layers of direct methanol fuel cells (DMFCs) are modified by *in situ* electropolymerization of *m*-aminobenzenesulfonic acid. By using electrochemical impedance spectroscopy and porosimetry, this modification is found to add polymer electrolyte into primary pores (<10 nm), where ionic resistance is high for lack of polymer electrolyte (*i.e.*, Nafion), and the additional electrolyte successfully decreases the ionic resistance by 10–15% compared to the plain carbon surface with a slight ion-conductivity (>40 kΩ cm). In view of methanol oxidation characteristics, this modification decreases the resistance by *ca.* 25% (from 5.1 Ω cm^2 to 3.7 Ω cm^2) at 0.6 V *vs.* DHE, resulting in the increase in the cell voltage of DMFC test by *ca.* 20 mV. The clear relation between the performance and the microstructures is concluded to be helpful to understand the performance of fuel cell electrodes in detail.

1. Introduction

For the successful exploitation of polymer electrolyte fuel cells (PEFCs), reduction of the loading of precious metal catalyst is of great importance, and thus numerous efforts have been devoted to improve their catalyst layers. The catalyst layers are generally prepared by two methods: (i) casting a mixture of catalyst nanoparticles (*e.g.*, carbon-supported Pt) and a polymer electrolyte (*e.g.*, Nafion) directly onto a gas diffusion layer (*e.g.*, carbon paper) [1–3]; (ii) casting the mixture once onto a PTFE sheet followed by decal transferring onto a Nafion membrane [2,4]. These layers contain some ineffective catalysts for the lack of three phases necessary for the reaction: electron-transfer phase (*e.g.*, carbon support, catalysts), mass-transfer phase (*e.g.*, pores) and ion-transfer phase (*e.g.*, polymer electrolyte). This unfavorable condition is caused mainly by the electrode microstructure composed of catalyst agglomerates, which are covered with a polymer electrolyte, and pores, which can be classified into two types: "primary pores", *i.e.*, those inside the agglomerates of Pt/C particles, and "secondary pores", *i.e.*, those between the agglomerates [4–6]. Thus, to increase the catalyst utilization efficiency, effective development based on precise understanding of the microstructure of the catalyst layers is necessary.

Since polymer electrolyte (*i.e.*, ion-transfer phase) in the catalyst layers has been reported to exist mainly in the secondary pores, catalysts inside primary pores are regarded to promote the reactions hardly for lack of ion-transfer phase. Therefore, the effective region for the catalytic reactions is formed at the wall of the secondary pores, while hardly formed in the primary pores [6]. In this respect, considerable efforts have been devoted to improve the ionic conductivity in the catalyst layers: for example, (i) improvements in compositions and preparation methods of the catalyst layers [2,4,5]; and (ii) modification of carbon supports with acidic groups [7–10]. These approaches appear to be effective in view of the practical application, however, the origin of the performance improvement is still open to debate, because these methods probably results in the different microstructures (*e.g.*, pore size and distribution of electrolyte).

This study describes an approach to add ion-conductive polymer to that portion of catalyst layers where polymer electrolyte does not exist intrinsically, and then the modified layers are analyzed to evaluate the influence of increase in the ionic conductivity of primary pores without changing microstructures, *e.g.*, the size of catalyst agglomerates. In this view, *in situ* electropolymerization of *m*-aminobenzenesulfonic acid (*m*-ABS), *i.e.*, a kind of self-doped polyanilines [11,12], was applied to add polymer electrolyte even into primary pores. The advantages of this treatment were: (i) the monomer is expected to penetrate even nanopores where intrinsic conductivity is insufficient for lack of Nafion; (ii) electropolymerization can generate a polymer electrolyte from electrode surface, *i.e.*, reaction on the electrode surface without Nafion is preferred;

* Corresponding author. Tel.: +81 3 5286 3202; fax: +81 3 3205 2074.
E-mail address: osakatets@waseda.jp (T. Osaka).
[1] http://www.tomi-s@suou.waseda.jp.

0378-7753/$ – see front matter © 2009 Elsevier B.V. All rights reserved.
doi:10.1016/j.jpowsour.2009.03.016

and (iii) the modification to catalyst layers is expected not to degrade electronic conductivity of the layer. Since electrooxidation of such an aromatic amine is known to bond its amino-group covalently to electrode surface (*e.g.*, carbon) [13,14], some portions of the electropolymerized *m*-ABS are expected to bond to the carbon surface. This fundamental approach is regarded to be suitable for understanding fuel cell catalyst layers.

2. Experimental

2.1. Electrode preparation

Two types of catalyst layers and a porous carbon-electrode were used. The catalyst layers were (i) a commercially available fuel cell electrode without intrinsic polymer electrolyte (1 mg cm^{-2} of Pt, 40 wt.% Pt/C, ElectroChem Inc.) and (ii) a typical catalyst layer containing Nafion ionomer (*ca.* 1.7 mg cm^{-2} Pt). The latter was prepared according to the following procedures: (a) Pt/C (HiSPEC^{TM} 11100, 70 wt.% Pt/C, Johnson Matthey), Nafion ionomer (5 wt.% solution, Aldrich) and ethyleneglycol dimethyl ether (EGDE) were mixed at a weight ratio of 8.6:3:120 (Pt/C:Nafion solution:EGDE) by following our previously published paper [1]; (b) this mixture was spray-coated onto a carbon paper (TGP-H-060 for anode, TGP-H-060T for cathode, Toray); (c) the carbon paper was dried at 130 °C in nitrogen atmosphere for 30 min.

The porous carbon-electrode was used to evaluate the influence of the weakly acidic groups, *e.g.*, carboxylic acid, to the ionic conductivity of the catalyst layers. The electrodes were prepared by knife-coating a mixture of carbon black (Vulcan XC72R, Cabot), a binder (Kyner2801: poly(vinylidene fluoride-co-hexafluoropropylene), PVdF-HFP, 10%-HFP, Tokyo Zairyo) and N-methylpyrolidinone at a weight ratio of 2.0 (carbon/binder) onto a carbon paper followed by drying first under ambient conditions and then at 120 °C for 30 min in nitrogen. The thickness of the carbon-black layer was *ca.* 50 μm.

2.2. Modification by electropolymerization

These catalyst layers were modified at room temperature by electropolymerization of *m*-ABS at 0.82 V *vs.* Ag/AgCl until the total charge reached *ca.* 3.5 C cm^{-2} to generate an excess amount of poly(*m*-ABS). To fill the pores of the electrode with aqueous solution, the electrode was presoaked in lower alcohol solution and then rinsed with an excess amount of pure water [15]. The electrochemical cell is a three-electrode configuration compartmentalized with a Nafion membrane (DuPont) between two compartments. One compartment contained 0.1 M *m*-ABS and 0.5 M Na_2SO_4, and a working electrode (*i.e.*, a catalyst layer) and a reference electrode (Ag/AgCl) was soaked in the solution. The other compartment contained only the supporting electrolyte, *i.e.*, 0.5 M Na_2SO_4 solution, and a counter electrode was soaked in the solution.

2.3. Evaluation of the electrodes without Nafion

The electrochemical properties of the electrodes filled with nitrogen-saturated pure water or 0.5 M sulfuric acid was evaluated in a two-electrode cell using a dynamic hydrogen electrode (DHE) [16] as a counter-and-reference electrode and a pretreated Nafion 112 membrane (DuPont) as the electrolyte. The DHE was prepared by casting a mixture of Pd/C (10 wt.%, Aldrich) and Nafion ionomer (5 wt.% solution, Aldrich) on a carbon paper (TGP-H-060, Toray), and operated under constant hydrogen-flow (20 mL min^{-1}) from a hydrogen generator (OPGU-2100S, Shimadzu). Electrochemical impedance spectroscopy (EIS) was performed at 0.4 V *vs.* DHE in the frequency range of 1 MHz–100 mHz with AC amplitude of 10 mV. Methanol oxidation characteristics in the absence of or in the presence of sulfuric acid (0.5 M) were evaluated by CV (0–1.0 V *vs.* DHE, 5 mV s^{-1}) in nitrogen-saturated 1 M methanol solution.

The EIS data thus obtained were analyzed using the following equation for the conventional transmission line model to analyze a porous electrode with an uniform ionic conductivity in the pores [17–19].

$$Z = \sqrt{\frac{R}{C(j\omega)^{\beta}}} \cdot \coth\sqrt{RC(j\omega)^{\beta}} + R_{\mathrm{bulk}} \quad (1)$$

where Z is the total impedance (Ω), R the ionic resistance for the electrode (Ω), C the double layer capacitance (F), β the exponent of constant phase element, and R_{bulk} is the bulk resistance mainly attributable to polymer electrolyte membranes (Ω).

In addition, the surface composition of the electrode with the modification was evaluated by X-ray photoelectron spectroscopy (XPS) (ESCA PHI-5400MC, PerkinElmer) applying Al Kα radiation (15 kV, 27 mA).

2.4. Evaluation of the electrodes with Nafion

The pore size distribution was determined by porosimetry (Belsorp mini, Bel Japan, Inc.) using nitrogen gas. These measurements were carried out after rinsing with an excess amount of pure water. The pore-size distribution was obtained as the BJH plots by analyzing the data of nitrogen adsorption–desorption isotherm.

The electrochemical properties of the modified electrode were evaluated using a membrane electrode assembly (MEA) consisting of a modified electrode for anode (1.7 mg cm^{-2} of Pt), an unmodified electrode for cathode (1.4 mg cm^{-2} of Pt) and a Nafion 115 membrane. These components were assembled by hot-pressing at 250 kgf cm^{-2} at 135 °C for 3 min.

The DMFC performance (*i.e.*, current–voltage curves) was evaluated using a galvanostat (HABF5001, Hokuto Denko) at room temperature (*ca.* 25 °C) in a commercially available cell (ElectroChem, Inc.) consisting of two graphite plates with flow channels (column flow pattern). The fuel and the oxidant were 1 M methanol (1 mL min^{-1}) and humidified oxygen (500 mL min^{-1}), respectively. The anode performance was evaluated by CV (0–0.8 V *vs.* DHE, 5 mV s^{-1}) and EIS (100 kHz–10 mHz, at 0.6 V *vs.* DHE) with supplying hydrogen (20 mL min^{-1}) to the cathode to work as a DHE. The EIS data of the catalyst layer containing Nafion, *i.e.*, the catalyst layer with primary pores and secondary pores, were analyzed by following our previously published method using an equivalent circuit assuming primary pores and secondary pores [1].

3. Results and discussion

3.1. Dependence of catalyst utilization efficiency on ionic resistance

First of all, the electropolymerization treatment was confirmed to generate an excess amount of poly(*m*-ABS), judged from the color change of the solution from transparent to purple [11]. XPS spectra (Fig. 1) show that this treatment was found to add some compounds containing sulfur- and nitrogen-groups, which did not exist in the untreated layer, into a catalyst layer without Nafion, this indicating that the some portion of polymerized *m*-ABS was successfully included in the layer. Since XPS can detect elemental composition near the surface ranging of a few nanometers in depth, the weak intensity may suggest that the poly(*m*-ABS) existed mainly inside the layer. This speculation can be supported by the following CV results and porosimetry results.

The influence of catalyst-layer electrolyte condition to degree of catalyst utilization was evaluated by using a catalyst layer without an intrinsic ion-conductor (*i.e.*, without Nafion ionomer). The

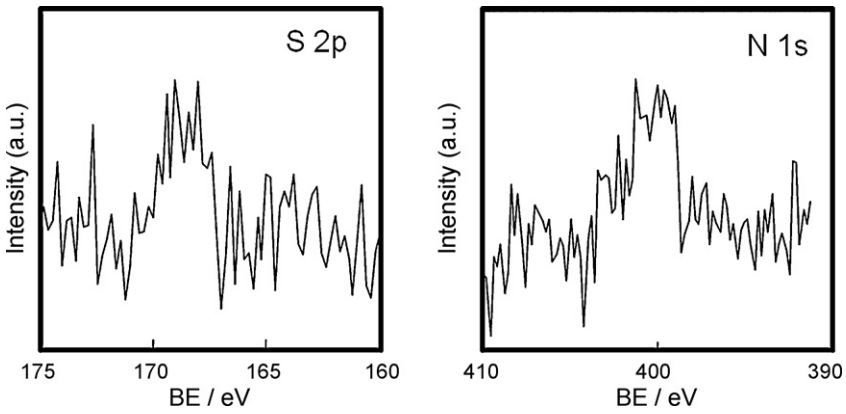

Fig. 1. Confirmation of the *m*-ABS modification by X-ray photoelectrone spectra on S-2p (left) and N-1S (right).

results of the layer filled with pure water (referred to as "Pt/C-PW") was compared with that obtained with the same layer filled with a sulfuric acid solution (referred to as "Pt/C-SA") and with that modified with poly(*m*-ABS) (referred to as "Pt/C-ABS"). The magnitude of methanol oxidation reaction (MOR) current on Pt/C-PW was totally different from that on Pt/C-SA (Fig. 2a) and that on Pt/C-ABS, *i.e.*, filling the pores with 0.5 M H_2SO_4 or poly(*m*-ABS) increased the current as expected from increase in ionic conductivity. The degree of catalyst utilization (the inset, Fig. 2a) was determined from the oxidation currents (*i.e.*, the current observed with Pt/C-PW or Pt/C-ABS was divided by that found with Pt/C-SA [20]). The values show that the degree of Pt/C-ABS was almost twice as high as that of Pt/C-PW, showing positive effect of the modification on the MOR characteristics. The degrees decreased with increasing electrode potential. This potential dependence is considered reasonable, because in general, faradaic reaction resistance decreases with increasing overpotential, whereas ionic resistance is independent on potential; thus the influence of ionic resistivity on MOR current is magnified by potential increase [20,21]. (The increase in the degree of catalyst utilization in the potential range of 0.6–0.8 V is attributable to diffusion limitation.)

The difference of MOR currents can be explained by comparing the EIS results (Fig. 2b). To evaluate the ionic resistivity precisely, the data were obtained in the absence of methanol to prevent potential dependent reaction (*i.e.*, faradaic reaction) from occurring. Each of the spectra of Pt/C-PW and Pt/C-ABS has a linear behavior with a slope of ~45° in the high frequency region, which generally results from a high ionic resistivity in a porous electrode [17–19].

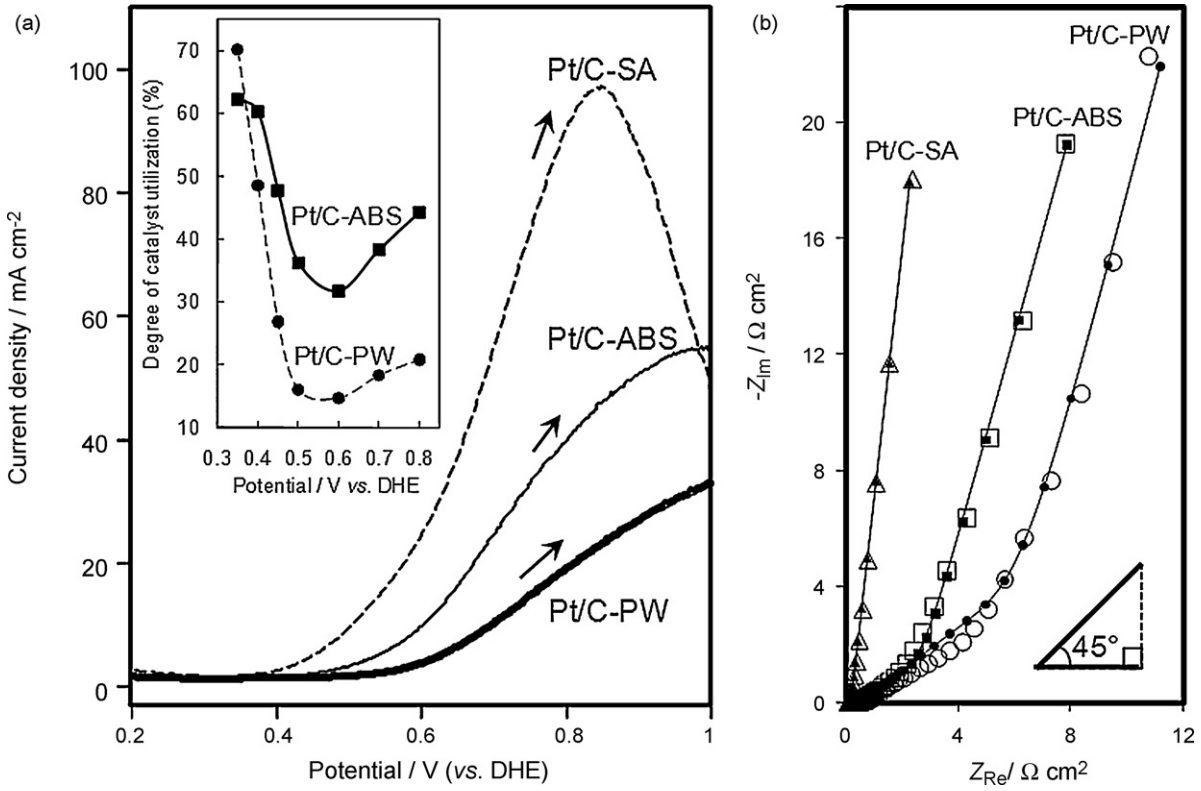

Fig. 2. Comparison of the characteristics of a catalyst layer without Nafion: (a) anodic scans of CVs for methanol oxidation in 1 M methanol at 5 mV s^{-1}. Bold line: a layer filled with pure water (Pt/C-PW); thin line: a layer modified with poly(*m*-ABS) (Pt/C-ABS); dashed line: a layer filled with 0.5 M sulfuric acid (Pt/C-SA). The inset is the degree of catalyst utilization for Pt/C-PW and Pt/C-ABS, calculated from the magnitude of oxidation currents (current ratio of these electrodes to Pt/C-SA). (b) Complex-plane impedance diagrams in the absence of methanol (circle dots: Pt/C-PW, square dots: Pt/C-ABS, triangle dots: Pt/C-SA). The filled dots are the experimental data, and the open dots are the calculated ones. AC amplitude: 10 mV. Frequency range: 1 MHz–0.1 Hz. DC bias: 0.4 V *vs.* DHE.

Table 1
Electrochemical properties of a catalyst layer without Nafion.[a].

Catalyst layers[b]	Ionic resistance, R/kΩ cm	Capacitance, C/F cm^{-3}	Bulk resistance, R_{bulk}/Ω cm^2	Exponent of CPE, β
Pt/C-SA	0.057	15	0.3	0.93
Pt/C-ABS	1.0	13	1.9	0.82
Pt/C-PW	2.7	12	2.0	0.84

[a] This analysis was based on a conventional transmission line model.
[b] The thickness of the porous layer was 55 μm measured using a micrometer.

The experimental plots were confronted with the theoretical values calculated with Eq. (1), and the theoretical values are summarized in Table 1. The ionic resistivity of Pt/C-PW was about 48 times as high as that of Pt/C-SA. The low value for Pt/C-SA is consistent with the values reported to be appropriate for fuel cells (<100 Ω cm) [2,19,22,23], and thus the large current obtained for Pt/C-SA is considered reasonable. The ionic resistivity of Pt/C-ABS was found to be one-third of that of Pt/C-PW, this clearly showing a positive effect of the modification with poly(*m*-ABS) on ionic resistance. Thus, the increase in the MOR current was attributable to the decrease in the ionic resistance.

The high resistance of Pt/C-PW probably caused a decrease in the effective surface area, resulting in the smaller MOR current. However, the resistivity of Pt/C-PW is ~1000 times less than that of pure water (18 MΩ cm). This unreasonably small resistivity is probably attributable to the ionic conductivity of the binder material and/or the carbon surface of the catalyst support, thus, to discuss the catalyst-layer conductivity in detail, detailed analysis on this respect is required.

3.2. Evaluation of ionic conductivity of carbon supports

The carbon surface is considered to be slightly ion-conductive originating from its weakly acidic groups, *e.g.*, carboxylic acid, thus, detailed electrochemical properties, especially ionic conductivity, of carbon particles were evaluated by using CV and EIS. To clarify the electrochemical response from the carbon surface in fuel-cell electrodes, the CVs recorded with a porous carbon-electrode in pure water (referred to as "C-PW") and in 0.5 M sulfuric acid (referred to as "C-SA") are shown in Fig. 3a. The CV of C-SA (dashed line) shows a typical capacitive behavior, while the CV of C-PW (solid line) shows a potential-dependent behavior which is similar to that reported by Liu et al. in the case of the use of a similar electrochemical cell [24]. The two CVs in Fig. 3a suggest that the capacitance of the electrode in pure water decreases with increasing potential.

These results can be interpreted by comparing with the EIS results presented in Fig. 3b. The EIS results also show potential dependence. The EIS data were analyzed using Eq. (1), and the calculated values are summarized in Table 2. This table clearly shows potential dependencies of capacitance and resistance for the porous carbon electrode in pure water (C-PW). The resistance was confirmed to be so high (*i.e.*, >40 kΩ cm) as to prevent the smooth reaction, and was found to increase several times with potential. This potential dependence of the resistance probably resulted from the potential dependence of the amount of ionic species. For example, it has been reported that the redox reaction of quinone/hydroquinone occurs on a carbon electrode at about 0.6 V [24,25]. At potentials lower than 0.6 V, the carbon surface attracts a greater amount of ionic species such as the protons dissociated from hydroquinone molecules. The capacitance was found to decrease with increasing potential, this also probably resulting from the potential dependence of the amount of ionic species. As Boo et al. reported [26], electrical double layers in nanopores are considered to vanish in a highly dilute electrolyte, based on Stern's model [27,28]. That is, the carbon electrode probably became free from ions at high potential, and hence the capacitance decreased due to the absence of electrical double layer in nanopores. These considerations are supported by the result that the carbon-electrode in sulfuric acid solution (C-SA) did not show potential dependence.

Here we conclude that the carbon surface of fuel-cell catalyst layer is slightly ion-conductive and the amount of ion-conductive groups is dependent on electrode potential. This behavior can be an

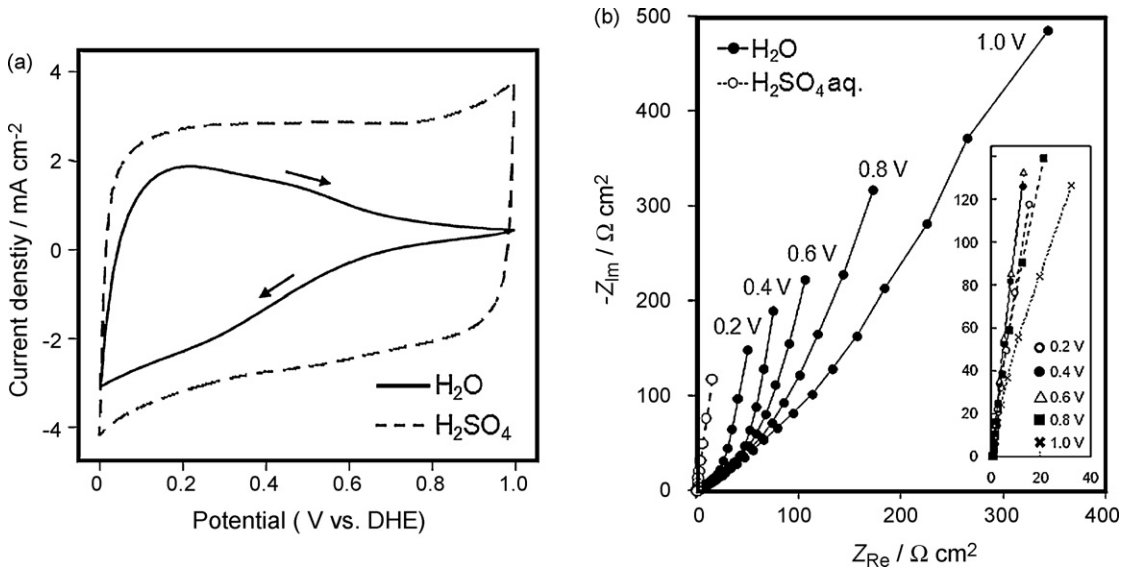

Fig. 3. Electrochemical characterization of a porous carbon-electrode in pure water (solid line) and in 0.5 M sulfuric acid (dashed line): (a) CVs recorded at 200 mV s^{-1}. The CV in pure water clearly shows a potential-dependent behavior. (b) Complex-plane impedance diagrams at different potentials. The data in pure water also show dependency on potential. The inset is the data for 0.5 M sulfuric acid and shows that the potential dependency was relieved by adding electrolyte. AC amplitude: 10 mV. Frequency range: 1 MHz–0.1 Hz.

Table 2
Electrochemical properties of porous carbon-electrodes containing different ionic conductors.[a].

Electrodes[b]	Potential, E/V *vs.* DHE	Ionic resistance, R/kΩ cm	Capacitance, C/F cm^{-3}	Bulk resistance, R_{bulk}/Ω cm^2	Exponent of CPE, β
C-PW (pure water)	0.2	40	2.1	1.2	0.85
	0.4	90	1.6	1.2	0.88
	0.6	115	1.3	1.2	0.86
	0.8	140	0.9	1.2	0.79
	1.0	140	0.5	1.2	0.67
C-SA (sulfuric acid)	0.2	0.13	2.6	0.67	0.94
	0.4	0.13	2.5	0.67	0.95
	0.6	0.14	2.3	0.67	0.95
	0.8	0.13	2.2	0.67	0.95
	1.0	0.13	2.3	0.67	0.94
C-ABS (poly(*m*-ABS))	0.2	26	4.2	1.2	0.87
	0.4	30	4.6	1.2	0.87
	0.6	37	4.5	1.2	0.87
	0.8	51	2.9	1.2	0.86
	1.0	72	2.1	1.2	0.85

[a] This analysis was based on a conventional transmission line model.
[b] The thickness of the porous layer was 50 μm measured using a micrometer.

indicator of the existence of electrode surface lacking in electrolyte. Since the carbon voltammograms show large currents in the potential range of 0–0.4 V, where hydrogen adsorption/desorption takes place in the case of a Pt electrode, this behavior of the carbon electrode possibly led the investigators to the misinterpretation that the voltammograms of Pt/C electrodes even filled with pure water show large response from Pt surface. This unreasonably large response has been attributed to hydrogen transport on the carbon surface (so-called "hydrogen spillover" [24,29,30]), thus, further detailed analyses may be required to conclude this respect.

The treatment with *m*-ABS changed the trace of the voltammogram of the carbon electrode (referred to as "C-ABS") as shown in Fig. 4a. The apparent reduction of capacitive current above 0.6 V was relieved, *i.e.*, the modification is considered to add electrolyte into pores of the electrode effectively. In addition, the weak oxidation peak at ~0.7 V and the weak reduction peak at ~0.3 V can be attributed to the redox response from poly(*m*-ABS), which is an electrochemically reactive polymer. To analyze the details of the influence of the modification on the ionic conductivity, EIS was applied. The complex-plane impedance diagrams are shown in Fig. 4b, and the parameters obtained from the fitting procedure using Eq. (1) are summarized in Table 2. It was found that the ionic resistance values (inset, Fig. 4b) decreased compared with those without the modification, though the potential dependence still remained slightly.

Even in the case of the layer with the modification, the ionic resistance was concluded too high. However, in primary pores, where the ion-transfer distance is considered to be less than several hundred nanometers, the areal resistance will become small enough for the fuel-cell reactions, *e.g.*, 1.2 Ω cm^2 (the distance: 100 nm) at 0.6 V for carbon electrode (see Table 2). In this view, some portion of the catalysts in primary pores can contribute to the reactions because of the slight conductivity of carbon surface. Thus, we investigated the catalyst layers with Nafion next.

3.3. Addition of ionic conductivity to catalyst layers with Nafion

Polymer electrolyte was added to the catalyst layer containing Nafion, especially into the pores lacking in polymer electrolyte. The nitrogen adsorption–desorption isotherms (Fig. 5a) were different

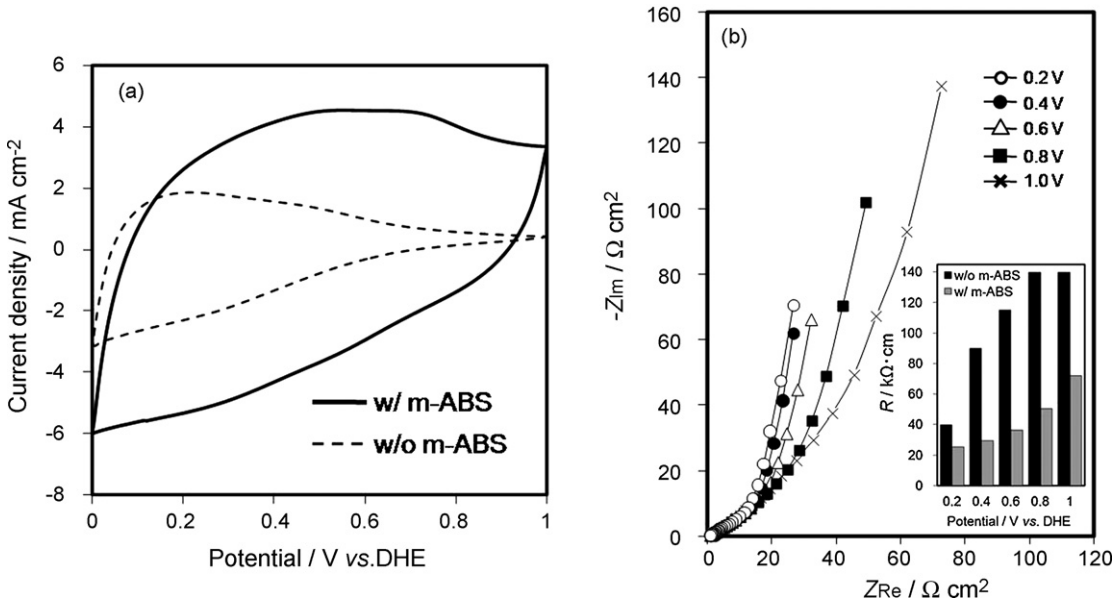

Fig. 4. Electrochemical characterization of a porous carbon-electrode modifed by *in situ* electropolymerization of *m*-ABS. The characteristics were evaluated in pure water. (a) Comparison of CVs of a carbon electrode with (solid line) and without (dotted line) the modification. Scan rate: 200 mV s^{-1}. (b) Complex-plane impedance diagrams at different potentials. The inset shows ionic resistance in the electrode obtained by fitting procedure. AC amplitude: 10 mV. Frequency range: 1 MHz–0.1 Hz.

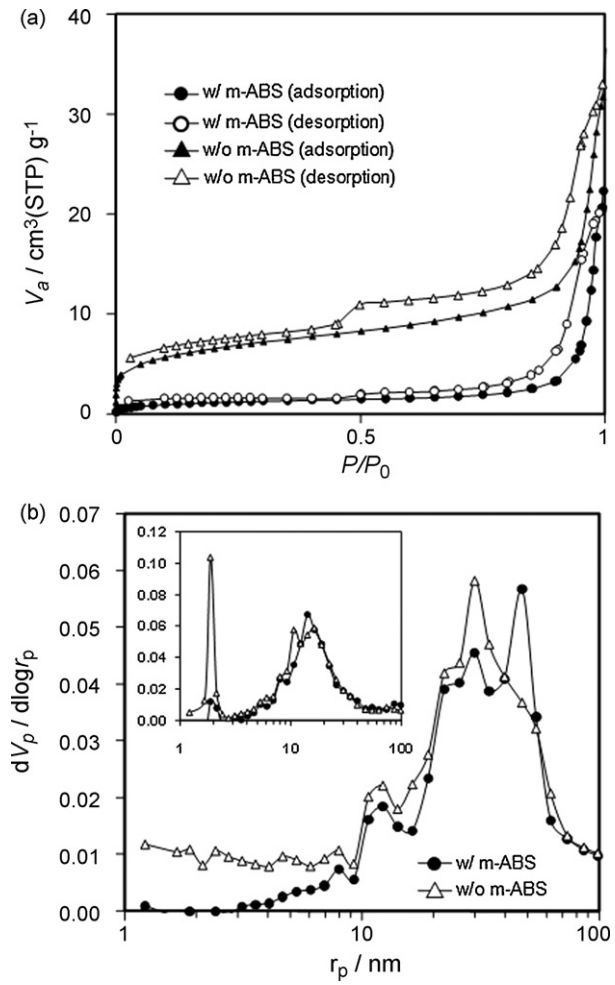

Fig. 5. Influence of the polymerized *m*-ABS on the pore volumes of catalyst layers containing Nafion. The triangular dots and the circular dots show the results of the sample without and with the modification, respectively. (a) Nitrogen adsorption–desorption isotherms. (b) Pore-size distribution (the BJH plots). r_p and V_p mean pore radius (nm) and pore volume (cm^3 g^{-1}), respectively. The inset was the bottleneck-size distribution obtained from the desorption isotherms.

between the layer with and without the modification. From these isotherms, pore-size distribution of the BJH plots (Fig. 5b) was obtained and showed that the layer without the modification has pore-volume mostly in the 10–100 nm range and partly in the <10 nm range. The bottleneck-size distribution from the nitrogen desorption isotherms (the inset, Fig. 5b) shows a bimodal distribution with its peaks at *ca.* 20 nm and *ca.* 2 nm. In this view, the pores in the <10 nm range can be regarded as primary pores, the pores in the catalyst agglomerates, and the pores in the 10–100 nm range can be regarded as secondary pores, the pores between the agglomerates. These pores are relatively small compared with those so far reported [5,6], probably resulting from the difference in preparation procedures [4]. Even in these small primary pores (<10 nm), the modification was found to add polymer electrolyte, judged from the significant decrease in the volume in the range of <10 nm, while the volume of secondary pores where the catalyst surface coated with Nafion did not change. Thus, the modification is expected to increase ionic conductivity of primary pores lacking in Nafion, without significant inhibition of mass-transfer in secondary pores.

The influence of the polymer electrolyte addition into primary pores were discussed in terms of the methanol oxidation characteristics (Fig. 6a), the DMFC performance (Fig. 6b), and the EIS results (Fig. 6c). The voltammograms (Fig. 6a) show that the modification increased the MOR current by ~40% (at 0.6 V) from *ca.* 9.7 mA cm^{-2} to *ca.* 13.6 mA cm^{-2}. This increase in the MOR current indicates that the additional electrolyte in primary pores increased the amount of effective catalysts by ~40%, which in turn resulted in the potential shift by *ca.* 25 mV to lower potential (the inset, Fig. 6a). This slight shift in anode potential was reproducibly confirmed even in the case of the DMFC test as shown in Fig. 6b, though its influence on the total performance is not significant.

This increase in the MOR current was analyzed using EIS, and the obtained data were analyzed based on the equivalent circuit assuming primary pores and secondary pores [1]. The obtained values summarized in Table 3 clearly show that the modification successfully added electrolyte into the region lacking in intrinsic electrolyte, judged from the decrease in the ionic resistances both in primary pores (R_{i1}) and in secondary pores (R_{i2}). The increase in the capacitance (C) is attributable to the increase in the electrochemically available surface area, but it may be attributed also to the capacitive response from the electrochemically active polyaniline backbone of poly(*m*-ABS). One may wonder that the decrease in the ionic resistance of primary pores is too small to decrease the total impedance effectively, but this small difference in ionic resistance can be attributed to the fact that this analysis is based on the use of constant resistances associated with the methanol oxidation reaction, *i.e.*, neglect of current concentration into highly ion-conductive region, leading to a smaller value of ionic resistance than that of actual one. For this reason, the decrease in the reaction resistance (R_{ct1}) probably reflects the increase in the effective catalysts due to the decrease in ionic resistance. (The increases in the impedances associated with the adsorbed intermediates

Table 3
Parameters of catalyst layers containing Nafion with and without the modification.[a]

Catalyst layers[b]	Primary pore resistance, R_{i1}/Ω cm^2	Secondary pore resistance, R_{i2}/Ω cm	Capacitance, C/F cm^{-3}	Exponent of constant phase element, β_1
w/o modification	0.20	90	15	0.84
w/ modification	0.17	75	18	0.92

Methanol oxidation reaction resistance, R_{ct1}/Ω cm^2	Intermediate oxidation resistance, R_{ct2}/Ω cm^2	Pseudo-inductance associated with adsorbed intermediate, L_1/H cm^2	Secondary pore fraction of reaction sites, θ
5.1	6.8	150	0.33
3.7	11	280	0.33

Bulk resistance, R_{bulk}/Ω cm^2	Inductance associated with noise[c], L_2/μH cm^2	Exponent of constant phase element to the noise[c], β_2
1.2	11	0.83
1.2	12	0.82

[a] This analysis was based on the equivalent circuit assuming primary pores and secondary pores.
[b] The thickness of the porous layer was 40 μm measured using a micrometer.
[c] The inductive noise observed in the high frequency region was analyzed using an impedance, $L_2(j\omega)^{\beta 2}$.

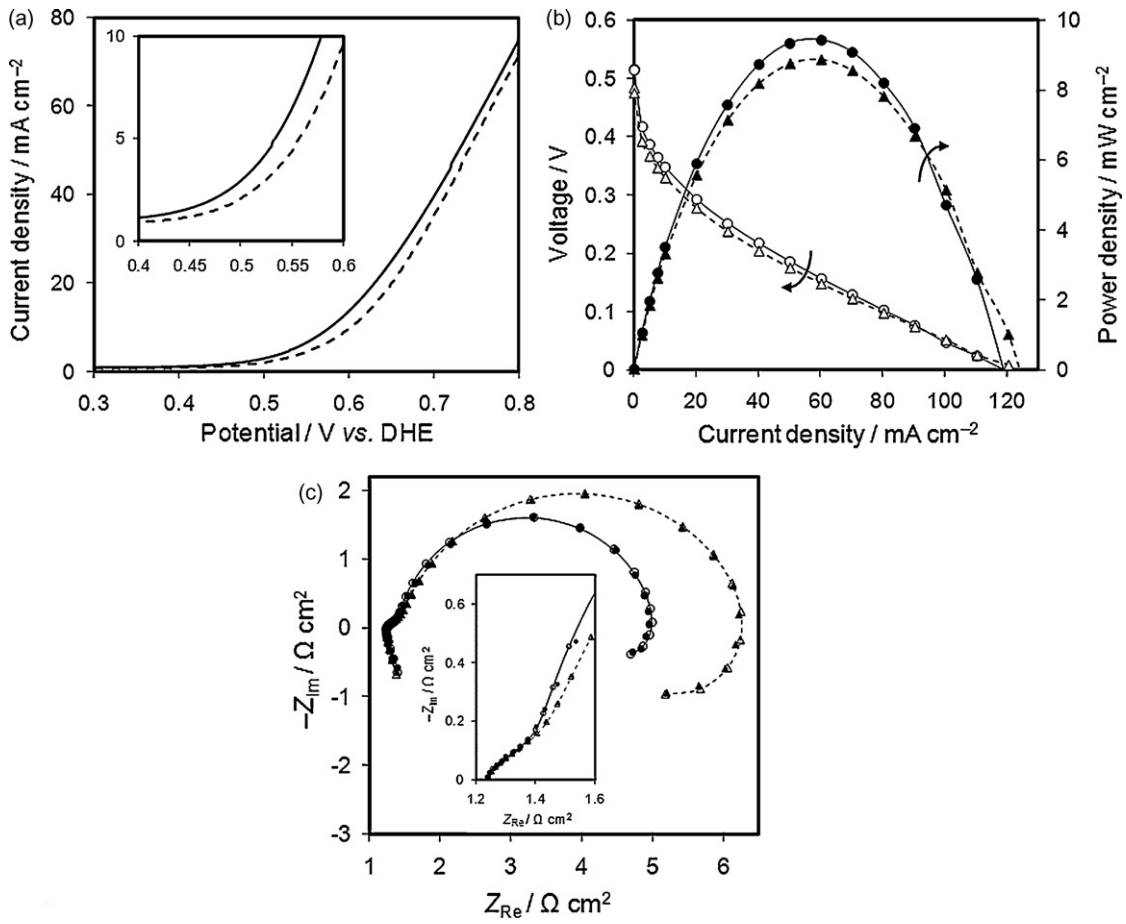

Fig. 6. Influence of the *m*-ABS modification on the performance of catalyst layers containing Nafion. (a) Anodic scans of CVs for methanol oxidation reaction on an electrode with (solid line) or without (dotted line) the modification at 5 mV s^{-1} in the range of 0–0.8 V *vs.* DHE. (b) DMFC performance of MEAs consisting of an anode with (circle dots) and without (triangle dots) the modification. The open dots show the current–voltage curves (3 min/point) at 25 °C. The filled dots show the current–power curves. (c) Complex-plane impedance diagrams for the methanol oxidation on the layer with (circular dots) and without (triangular dots) the modification. The filled dots and the open dots respectively show the experimental data and the calculated data. The inset is magnified diagrams in the high frequency region. Frequency: 100 kHz–10 mHz. DC bias: 0.6 V *vs.* DHE.

maybe originated from the fact that the intermediate reaction has a chemical step, *i.e.*, surface diffusion of adsorbed OH groups, and the impedance may be increased with applied current, but further detailed analysis is required to conclude this point.)

4. Conclusion

The modification of DMFC catalyst layers, *i.e.*, *in situ* electropolymerization of *m*-ABS, surely added ion-conductors even into primary pores (<10 nm), resulting in the improvement in the methanol oxidation characteristics. The decrease in the ionic resistance was not significant (10–15%), but it obviously decreased the methanol oxidation resistance by *ca.* 25%. In view of cell performance, this modification reproducibly increased the voltage by *ca.* 20 mV. This clear relation between the microstructure and the performance is helpful to understand the performance of fuel cell electrodes in detail.

Acknowledgements

This work was partly supported by the Grant-in-Aid for Specially Promoted Research "Establishment of Electrochemical Device Engineering", by the Global COE Program "Center for Practical Chemical Wisdom" and by Encouraging Development Strategic Research Centers Program "Establishment of Consolidated Research Institute for Advanced Science and Medical Care" from the Ministry of Education, Culture, Sports, Science and Technology (MEXT), Japan.

References

[1] S. Tominaka, N. Akiyama, T. Momma, T. Osaka, J. Electrochem. Soc. 154 (2007) B902–B909.
[2] S.S. Kocha, Handbook of Fuel Cells: Fundamentals Technology and Applications, John Wiley & Sons, England, 2003 (Chapter 43).
[3] M. Uchida, Y. Fukuoka, Y. Sugawara, N. Eda, A. Ohta, J. Electrochem. Soc. 143 (1996) 2245–2252.
[4] J. Xie, K.L. More, T.A. Zawodzinski, W.H. Smith, J. Electrochem. Soc. 151 (2004) A1841–A1846.
[5] J.M. Song, S. Suzuki, H. Uchida, M. Watanabe, Langmuir 22 (2006) 6422–6428.
[6] M. Uchida, Y. Aoyama, N. Eda, A. Ohta, J. Electrochem. Soc. 142 (1995) 4143–4149.
[7] H. Kuroki, T. Yamaguchi, J. Electrochem. Soc. 153 (2006) A1417–A1423.
[8] Z.Q. Xu, Z.G. Qi, A. Kaufman, Electrochem. Solid State Lett. 6 (2003) A171–A173.
[9] G. Selvarani, A.K. Sahu, N.A. Choudhury, P. Sridhar, S. Pitchumani, A.K. Shukla, Electrochim. Acta 52 (2007) 4871–4877.
[10] Z.Q. Xu, Z.G. Qi, A. Kaufman, Electrochem. Solid State Lett. 8 (2005) A313–A315.
[11] A. Kitani, K. Satoguchi, H.Q. Tang, S. Ito, K. Sasaki, Synth. Met. 69 (1995) 129–130.
[12] A. Malinauskas, J. Power Sources 126 (2004) 214–220.
[13] A. Adenier, M.M. Chehimi, I. Gallardo, J. Pinson, N. Vila, Langmuir 20 (2004) 8243–8253.
[14] X.F. Li, Y. Wan, C.Q. Sun, J. Electroanal. Chem. 569 (2004) 79–87.
[15] T.R. Ralph, G.A. Hards, J.E. Keating, S.A. Campbell, D.P. Wilkinson, M. Davis, J. St-Pierre, M.C. Johnson, J. Electrochem. Soc. 144 (1997) 3845–3857.
[16] A. Kuver, I. Vogel, W. Vielstich, J. Power Sources 52 (1994) 77–80.
[17] R. de Levie, Electrochim. Acta 8 (1963) 751.
[18] J.M. Elliott, J.R. Owen, Phys. Chem. Chem. Phys. 2 (2000) 5653–5659.

[19] R. Makharia, M.F. Mathias, D.R. Baker, J. Electrochem. Soc. 152 (2005) A970–A977.
[20] K. Mund, F.V. Strum, Electrochim. Acta 20 (1975) 463–467.
[21] J. Divisek, R. Jung, I.C. Vinke, J. Appl. Electrochem. 29 (1999) 165–170.
[22] C. Boyer, S. Gamburzev, O. Velev, S. Srinivasan, A.J. Appleby, Electrochim. Acta 43 (1998) 3703–3709.
[23] G. Li, P.G. Pickup, J. Electrochem. Soc. 150 (2003) C745–C752.
[24] W.-J. Liu, B.-L. Wu, C.-S. Cha, J. Electroanal. Chem. 476 (1999) 101–108.
[25] K. Kinoshita, J.A.S. Bett, Carbon 11 (1975) 403–411.
[26] H. Boo, S. Park, B. Ku, Y. Kim, J.H. Park, H.C. Kim, T.D. Chung, J. Am. Chem. Soc. 126 (2004) 4524–4525.
[27] C.-H. Hou, C. Liang, S. Yiacoumi, S. Dai, C. Tsouris, J. Colloid Interf. Sci. 302 (2006) 54–61.
[28] A.J. Bard, L.R. Faulkner, Electrochemical Methods: Fundamentals and Applications, 2nd ed., John Wiley & Sons, Inc., New York, 2001, pp. 534–554.
[29] J.H. Jiang, B.L. Yi, J. Electroanal. Chem. 577 (2005) 107–115.
[30] J. Mcbreen, J. Electrochem. Soc. 132 (1985) 1112–1116.